

MASTER

CONVOY ELECTRON PRODUCTION IN POLYCRYSTALLINE AND MONOCRYSTALLINE TARGETS

Sven Hultd

University of Tennessee, Knoxville TN 37916, and
Oak Ridge National Laboratory, Oak Ridge TN 37830

Summary

The velocity distribution of electrons ejected close to the forward direction by 0.8-2 MeV/A ions traversing various solid targets, including a Au monocrystal, is measured in coincidence with emerging charge-selected ions.

The velocity spectrum is observed to be independent of outgoing projectile velocity and charge state for polycrystalline targets. Measurements on the Au crystal under channeling conditions show dependences on final charge state, and are tentatively explained by assuming that the main contribution to the production yield comes from the non-channelled fraction of the ions. A simple model for the creation of the forward-ejected electrons is proposed, which accounts for most of the experimental findings.

Introduction

Fast ions penetrating solids or gases produce free electrons, whose velocity distribution shows a distinct peak centered at the velocity of the emerging projectile.^{1,2} Since a dominant influence on the electron momentum distribution comes from the Coulomb field of the emerging ion, in the ion-atom case the electron production is often ascribed to electron capture to the continuum. In the solid target case, the electrons are commonly referred to as convoy electrons (CE).⁶

For continuum electron production in gases under single collision conditions a distinction can be made between the mechanism in which one of the electrons of the projectile is excited to a low-lying continuum state (electron loss to the continuum, ELC), and that in which a target electron is captured with a velocity close to that of the ion (electron capture to the continuum, ECC). The velocity spectrum of electrons ejected in the forward direction shows, in the case of a dominant contribution from the ELC channel, a symmetric peak with width almost independent of projectile velocity,³ while in collisions where ECC dominates (as for incident bare ions) the width is observed to be roughly proportional to the projectile velocity, in qualitative accordance with predictions.⁴

The situation is less clear for dense targets, in which the state of the ion at the time of creation of the electron is unknown. Models assuming collisions near the surface as the source for convoy electrons may sometimes be justified by the short mean free path for keV electron scattering inside solids, which may limit the possible origin to the last ~ 10 Å of the target.

Alternatively, a bulk production mechanism has been proposed.^{5,6} Ions traveling in solids with velocity

$$v_i > v_F = (2E_F/m)^{1/2}, \quad (1)$$

where E_F is the Fermi energy of the material and m the electron mass, are trailed by a spatially oscillating (wake) potential,⁷ caused by collective motions of the target electrons. This velocity is of the order of 1 atomic unit (a.u.) for most materials. The amplitude

of the oscillations for $v_i \sim 2-20$ a.u. ions in metals is estimated to be sufficiently strong to bind valence electrons from the target in a wake-riding state with a mean free path for the decay of $10-20$ Å.^{7,8} These wake-bound electrons may eventually penetrate the exit surface and emerge with velocity close to v_i , and thus contribute to the convoy population.

Major sources of uncertainty in earlier experiments for lighter ions at lower velocities are the treatment of background and, for heavy projectiles, the averaging over final charge states. Since most experiments have been carried out with residual gas pressure larger than 10^{-3} Torr, there is also a possible influence of contaminating layers on the target surface which must be examined.

In recent experiments at ORNL we have tried to overcome these difficulties by detecting electrons in coincidence with the charge-selected ion and by interchanging polycrystalline targets with a single crystal, which can either be randomly oriented or aligned along one of its planar or axial channeling directions.

Experiment

Beams of pA intensity and various charge states were obtained from the ORNL tandem ($Z = 6, 8$; $E = 0.8 - 2$ MeV/A). Self-supporting foils of C ($30 \mu\text{g}/\text{cm}^2$), Al ($50 \mu\text{g}/\text{cm}^2$) and Au ($100 \mu\text{g}/\text{cm}^2$), and a Au monocrystal ($\sim 300 \mu\text{g}/\text{cm}^2$) were used as targets. For the beams used, charge-state equilibrium was reached in the foils.

The electron spectra were acquired with a spherical sector electrostatic analyzer, whose energy resolution was set to 1-1.4% (FWHM) by the source size and an aperture at the exit focus. The targets were placed at the entrance focus of the analyzer. The incident beam was collimated to 0.06 deg, so that $> 95\%$ of incident 1.25 MeV/A oxygen beams were within typical channeling acceptance angles, and the angular spread after the amorphous targets was dominated by the scattering in the foils. The half angle of the cone of observation, centered around the beam axis, was set to 1.5-1.7 deg. A hole in the outer plate of the analyzer permitted transmission of the emergent ion beam. The ions were subsequently focused by a quadrupole doublet, charge-state analyzed in a magnet, and collected in an electron multiplier (CEM), mounted in the end of a ~ 1 m long Faraday cup. Three sets of mutually orthogonal pairs of Helmholtz coils reduced the residual magnetic field in the region of observation to less than 10^{-6} T. A pressure of $\sim 10^{-7}$ Torr in the system eliminated charge-changing collisions with the residual gas. Data were normalized either to the charge collected in the Faraday cup, or to the number of ions counted by the CEM. Standard coincidence electronic techniques were used to measure the electron velocity distribution. A start signal for a time-to-amplitude converter was generated by the detection of an energy-analyzed electron, while the stop signal was generated by the arrival of the charge-selected ion in the Faraday cup CEM within the allowed time window. Accidental events were counted in a time window of equal width. The total ion flux was adjusted so that the true-to-accidentals ratio always exceeded 5. The set-up permitted simultaneous measurement of the number and energy distribution of electrons in coincidence with a particular

CONF-801111-221

DISCLAIMER

This book was prepared as an account of work sponsored by an agency of the United States Government. Neither the United States Government nor any agency thereof, nor any of their employees, makes any warranty, express or implied, or assumes any legal liability or responsibility for the accuracy, completeness, or usefulness of any information, apparatus, product, or process disclosed, or represents that its use would not infringe privately owned rights. Reference herein to any specific commercial product, process, or service by trade name, trademark, manufacturer, or otherwise, does not necessarily constitute or imply its endorsement, recommendation, or favoring by the United States Government or any agency thereof. The views and opinions of authors expressed herein do not necessarily state or reflect those of the United States Government or any agency thereof.

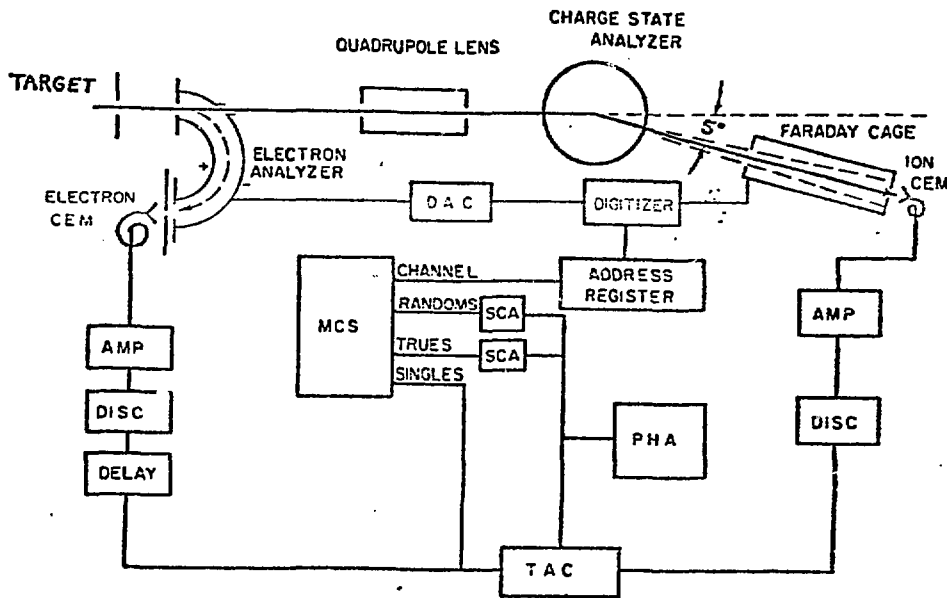


Figure 1. Schematic diagram of the experimental apparatus.

charge state of the emergent ion, and the total number of ions of a certain charge state. A schematic diagram of the set-up is shown in Figure 1.

Results

We find that in all the investigated cases the full width at half maximum (FWHM) of the convoy velocity peak from solid targets is nearly independent of projectile velocity and atomic number, of emerging charge state, and of the target chosen. The peaks are nearly symmetric with a slight skew corresponding to an enhancement of the $v_e > v_i$ wing (Figure 2).

For a given incident projectile and polycrystalline target the yield, defined as the number of CEs per emerging ion, does not depend on the charge state of the emerging ion, while the dependence on projectile atomic number and energy and on target is observed to be roughly

consistent with earlier measurements,⁹ in which the yields for the polycrystalline targets were observed to vary according to the expression:

$$Y = k \times C_{\text{targ}} \times Z_{\text{proj}}^m \times E^{-n}, \quad (2)$$

where E and Z_{proj} are the energy in MeV/A and atomic number of the projectile, $m = 2.75$ and $n = 2.25$. C is a target-dependent constant, ranging from 1 to 1.7 for the polycrystalline foils used, while an estimate of the average number of collisions inside the targets, as

given by a reduced thickness estimate,¹⁰ ranges from 1 to 50. An estimate of the absolute total yield similar to the one in Ref. 9 gives k of the order 10^{-3} , with E in MeV/A.

Yields for ions traversing channels in the Au crystal are all distinctly lower than those from polycrystalline targets and show a significant dependence on final charge state, as seen in Table 1. The highest yields are observed in cases where simultaneously single or double bound-state capture occurs, while the lowest are those for which the charge state decreases or does not change. A similar correlation between bound-state

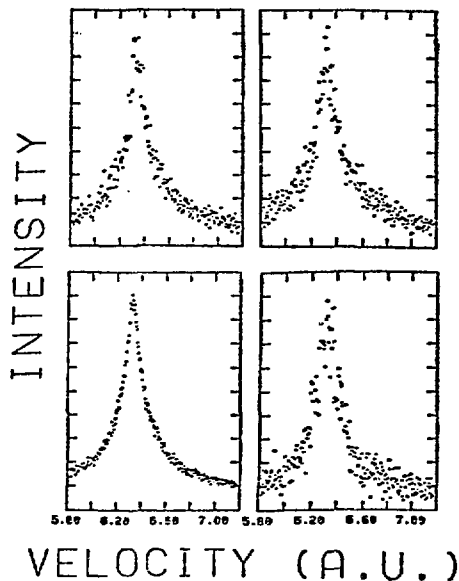


Figure 2. The longitudinal velocity distribution of convoy electrons emerging from a solid when 12 MeV $^{12}\text{C}^{2+}$ is incident on a 40 $\mu\text{g}/\text{cm}^2$ Al target. The "singles" or non-coincident distribution is shown in the lower left-hand corner. The electron velocity distributions in coincidence with the final charge state of C^{6+} , C^{4+} , and C^{3+} are shown in clockwise arrangement starting in the upper left-hand corner. The vertical scale (intensity) is arbitrarily normalized for each spectrum.

Table 1. Convoy electron yield (%) per emergent ion, for O^{8+} incident at 2.4 MeV/A on Au in the $\langle 110 \rangle$, $\langle 100 \rangle$, and random directions. The yield is normalized to the measured random yield of $\sim 3.8 \times 10^{-3}$ electrons/ion. The number in parentheses is the fraction (%) of emergent ions in state q_e .

q in	q_e out	q_e		
		8^+	7^+	6^+
8^+	$Y\langle 110 \rangle$	21 (68)	39 (28)	82 (4)
	$Y\langle 100 \rangle$	37 (59)	58 (35)	79 (6)
	$Y\langle \text{Rand} \rangle$	100 (26)	100 (59)	100 (15)
7^+	$Y\langle 110 \rangle$	29 (42)	24 (51)	58 (7)
	$Y\langle 100 \rangle$	37 (52)	47 (42)	71 (6)
	$Y\langle \text{Rand} \rangle$	100 (25)	100 (60)	100 (15)
6^+	$Y\langle 110 \rangle$	37 (31)	29 (42)	21 (27)
	$Y\langle 100 \rangle$	39 (49)	45 (42)	47 (9)
	$Y\langle \text{Rand} \rangle$	100 (27)	100 (57)	100 (16)

capture and capture to the continuum has been verified in experiments on Ar gas targets, where for 9 a.u.

O^{8+} incident ions, single or multiple bound-state capture is often observed to accompany ECC.

Discussion

The experimental finding that the spectrum shape is nearly symmetric and independent of the projectile atomic number and velocity suggests a close connection between convoy electron production and ELC processes in gaseous targets, and is inconsistent with both the "last layer" hypothesis of Dettmann et al.⁴ and with present wake-riding models^{11,12} (Figure 3).

Following the arguments of Sternglass¹⁴ on secondary electron emission, the weakness of the target dependence can be qualitatively explained. According to this model, the yield of secondaries is essentially determined by the ratio of the cross section for electron production to that for electron scattering inside the solid. This ratio is essentially the same for all conductors at a given projectile velocity and charge. The asymmetry of the convoy peak can be explained by assuming a velocity dependence of $v^{-1.6}$ for the probability of electron scattering away from the $v_e \approx v_i$ condition (Figure 4).

For the channeled ions a simple model can be constructed which produces most of the data. Two classes of ions are postulated, A and B, of which class A contains the "well-channeled" ions, while ions in class B experience close collisions with the target atoms. In the A channel the ions are confined to collisions with loosely bound outer electrons with energy ~ 10 eV, for which capture and loss cross sections are small, while the B ions interact with closely bound electrons, which are far more efficient at contributing to capture according to the Bohr velocity matching criterion. Assuming (as is indicated by the data) negligible yield for double bound + continuum state capture for class A ions, and a yield equal to that of the crystal in random direction for all class B ions, the fractions of ions in the different channels and the corresponding total yields can

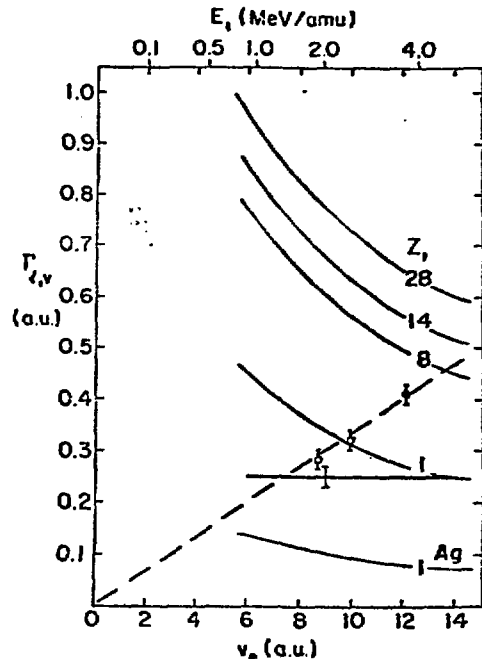


Figure 3. The full width at half maximum of the longitudinal electron velocity distribution, $\Gamma_{1/2}$, for convoy electrons as a function of the electron velocity v_e . The incident projectile energy, in MeV/u, appears at the top of the figure. The dashed line is the ECC prediction.³ The solid lines are the predictions of the wake-riding theory for an Al target with the indicated projectiles.¹¹ The lowest solid curve marked Ag is the prediction of wake-riding theory for protons incident on Ag. The experimental data for solids are represented by the heavy solid line. The open points represent the gaseous target (Ne and Ar) results for O^{8+} and Si^{14+} .

be inferred for all combinations of incoming and emerging charge states. Using these values and crystallographic data for the different channels, the effective area available for group A and B ions can be calculated. The result, for both the $\langle 110 \rangle$ and the $\langle 100 \rangle$ channels, is that only ions with impact parameter less than ~ 0.65 Å, which roughly corresponds to the mean radii of the 4f and 5p electron orbits in Au, appreciably contribute to convoy electron production.

Since the observation depth in any of the models considered does not exceed 10-20 Å, establishment of complete charge-state equilibrium following the CE creation is most unlikely. The total absence of correlation between yield or shape with emergent projectile charge state (for ions randomly scattered in monocrystals scattered in polycrystals) therefore leads to the suggestion that the CEs are created in conjunction with an unknown process which repopulates the charge states with probabilities equal to those for equilibrium, and thus may make the ion charge prior to the process inaccessible to experiment.

A relevant quantity for comparison of a possible charge dependence with theory is the average ion charge inside the target, a quantity which is incompletely

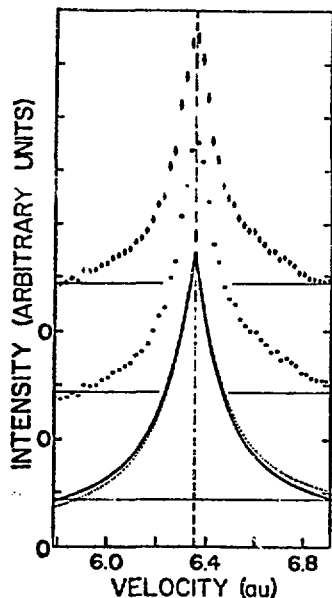


Figure 4. Spectrum of convoy electrons emergent near 0 deg from 16 MeV O^{3+} ions traversing a $30 \mu\text{g}/\text{cm}^2$ C foil. The upper data points are obtained from the raw spectrum (lower points), through a correction factor ($v_e^{-1.6}$, to account for the estimated velocity dependence of the electron escape depth. The lower curves represent respective fitted cusp shapes, which better display the degree of symmetrization produced.

known. The experimental results for channeled ions may require consideration of the fact that charge-state equilibrium is far from reached in these cases,¹⁵ leading to a possible dependence of yield on incoming charge state.

In conclusion, we summarize an admittedly incomplete, though useful, model for convoy electron production in polycrystalline solids: CE production is initiated in close collision with target atoms throughout the bulk, but those observed originate within $\sim 10 \text{ \AA}$ from the exit surface. First single or multiple electron capture occurs, immediately followed by electron loss to the continuum. Further subsequent influence of the Coulomb field of the ion on the velocity distribution is small.

Acknowledgements

The measurements have been carried out at Oak Ridge National Laboratory by the University of Tennessee/ORNL atomic physics group, especially I. A. Sellin, S. B. Elston, R. S. Thoe, M. Breinig, L. Liljeby, S. Huldt, S. D. Berry and G. A. Glass. The channeling experiments were performed with the kind help of S. Datz and S. Overbury, who also suggested their interpretation. Valuable participation of R. Laubert is also gratefully acknowledged.

This work was partially supported by the National Science Foundation; the Office of Naval Research; and the Fundamental Interactions Branch, Division of Chemical Sciences, Office of Basic Energy Sciences, U. S. Department of Energy, under contract W-7405-eng-26.

References

1. K. G. Harrison and M. W. Lucas, *Phys. Lett.* **33A**, 142 (1970).
2. G. B. Crooks and M. E. Rudd, *Phys. Rev. Lett.* **25**, 1599 (1970).
3. I. A. Sellin and R. Laubert, in *Proceedings of the Third International Workshop on Inelastic Ion-Surface collisions*, Munich, Germany, September 17-19, 1980, to be published.
4. K. Dettmann, K. G. Harrison, and M. W. Lucas, *J. Phys. B* **7**, 269 (1974).
5. F. Drepper and J. S. Briggs, *J. Phys. B* **9**, 2063 (1976).
6. W. Brandt and R. H. Ritchie, *Phys. Lett.* **62A**, 374 (1977).
7. R. H. Ritchie, W. Brandt and P. M. Echenique, *Phys. Rev. B* **14**, 4808 (1976).
8. M. Day and M. Ebel, *Phys. Rev. B* **19**, 3434 (1979).
9. R. Laubert, S. Huldt, M. Breinig, L. Liljeby, S. B. Elston, R. S. Thoe, I. A. Sellin, to be published in *J. Phys. B*.
10. L. Mayer and P. Krygel, *Nucl. Instr. Meth.* **98**, 381 (1972).
11. W. Meckbach, N. Arista, and W. Brandt, *Phys. Rev. Lett.* **65A**, 113 (1978).
12. M. Day, *Phys. Rev. Lett.* **44**, 752 (1980).
13. C. R. Vane, I. A. Sellin, S. B. Elston, M. Suter, R. S. Thoe, G. D. Alton, S. D. Berry, and G. A. Glass, *Phys. Rev. Lett.* **43**, 1388 (1979).
14. E. J. Sternglass, *Phys. Rev.* **108**, 1 (1957).
15. J. C. Ashley, C. J. Tong, and R. H. Ritchie, *Surface Science* **81**, 409 (1979).
16. S. Datz, F. W. Martin, C. D. Moak, B. R. Appleton, and L. B. Bridwell, in *Atomic Collisions in Solids IV*, ed. by S. Andersen (Gordon & Breach Science Publishers, 1972), p. 87.